npg

ORIGINAL ARTICLE

IFNβ/TNFα synergism induces a non-canonical STAT2/IRF9-dependent pathway triggering a novel DUOX2 NADPH Oxidase-mediated airway antiviral response

Karin Fink[1, 2], Lydie Martin[1, *], Esperance Mukawera[1, *], Stéfany Chartier[1], Xavier De Deken[3], Emmanuelle Brochiero[1, 4], Françoise Miot[3], Nathalie Grandvaux[1, 2]

[1]Centre de Recherche du CHUM (CRCHUM), Montréal, Québec, Canada H2X 1P1; [2]Department of Biochemistry, Faculty of Medicine, Université de Montréal, Québec, Canada H3T 1J4; [3]Institut de Recherche Interdisciplinaire en Biologie Humaine et Moléculaire, Université Libre de Bruxelles, Campus Erasme, 1070 Brussels, Belgium; [4]Department of Medicine, Faculty of Medicine, Université de Montréal, Montréal, Québec, Canada H3T 1J4

Airway epithelial cells are key initial innate immune responders in the fight against respiratory viruses, primarily via the secretion of antiviral and proinflammatory cytokines that act in an autocrine/paracrine fashion to trigger the establishment of an antiviral state. It is currently thought that the early antiviral state in airway epithelial cells primarily relies on IFNβ secretion and the subsequent activation of the interferon-stimulated gene factor 3 (ISGF3) transcription factor complex, composed of STAT1, STAT2 and IRF9, which regulates the expression of a panoply of interferon-stimulated genes encoding proteins with antiviral activities. However, the specific pathways engaged by the synergistic action of different cytokines during viral infections, and the resulting physiological outcomes are still ill-defined. Here, we unveil a novel delayed antiviral response in the airways, which is initiated by the synergistic autocrine/paracrine action of IFNβ and TNFα, and signals through a non-canonical STAT2- and IRF9-dependent, but STAT1-independent cascade. This pathway ultimately leads to the late induction of the DUOX2 NADPH oxidase expression. Importantly, our study uncovers that the development of the antiviral state relies on DUOX2-dependent H_2O_2 production. Key antiviral pathways are often targeted by evasion strategies evolved by various pathogenic viruses. In this regard, the importance of the novel DUOX2-dependent antiviral pathway is further underlined by the observation that the human respiratory syncytial virus is able to subvert DUOX2 induction.

Keywords: antiviral; cell signaling; innate immunity; inflammation; NADPH oxidase; interferon
Cell Research (2013) 23:673-690. doi:10.1038/cr.2013.47; published online 2 April 2013

Introduction

The mucosal linings of the airways are constantly exposed to an array of microbial pathogens including life-threatening respiratory viruses. Control of the host-microbe homeostasis at the mucosal epithelium is essential to prevent microorganism-triggered inflammatory diseases. In addition to acting as a physicochemical barrier, airway epithelial cells (AECs) are also responsible for key immune responses in the fight against viruses. AECs rapidly recognize invading respiratory viruses to actively trigger the production of antiviral substances including peptides and cytokines that limit invasion and spread of the pathogens. Additionally, AECs produce proinflammatory cytokines and chemokines, leading to immune cell recruitment and activation at the infection sites. Thus, the molecular pathways engaged upon viral infection of AECs and the resulting antiviral state are crucial for pathogen clearance and host recovery.

The current picture of the innate immune response proposes that in AECs, viral nucleic acids are sensed by pattern recognition receptors (PRRs) of the Toll-like receptor (TLR) and RIG-I-like receptor (RLR) families.

The downstream signaling cascades culminate into the activation of NF-κB and interferon regulatory transcription factor 3 (IRF-3), which regulate the expression of genes encoding proinflammatory cytokines such as tumor necrosis factor α (TNFα), and antiviral cytokines, primarily type I (α and β) and type III (λ1-3) interferons (IFNs) [1]. Secreted type I IFNs bind to their cognate receptors, interferon-α/β receptor (IFNAR), resulting in the activation of the JAK/STAT signaling pathway and the subsequent formation of the interferon-stimulated gene factor 3 (ISGF3) transcription factor complex composed of STAT1, STAT2 and IRF9. ISGF3 activation is a prerequisite for the establishment of a robust antiviral state through the induction of numerous interferon-stimulated genes (ISGs) encoding antiviral proteins that modulate protein synthesis, cell growth and apoptosis [2]. Understanding the molecular mechanisms underlying the establishment of the antiviral state in AECs is the focus of intensive researches aimed at identifying novel antiviral genes and their regulatory pathways.

The NADPH oxidase enzymes Dual Oxidase 1 and 2 (DUOX1 and DUOX2) originally identified in the thyroid have been shown to be expressed in mammalian epithelial tissues, including epithelial barriers constantly exposed to microbes, such as the respiratory and intestinal tracts [3]. Increasing evidence has been reported to support the role of DUOX1 and DUOX2 in host defense against bacterial invasion at mucosal surfaces through the generation of H_2O_2 [3, 4]. While *DUOX1* is induced following stimulation with IL-4 and IL-13, typical T helper (Th) 2 cytokines, *DUOX2* is induced by the Th1 cytokine IFN-γ [5]. Additionally, *DUOX2* is upregulated following infection with rhinovirus (RV) or *Paramyxoviridae* viruses, and in response to stimulation with polyinosine-polycytidylic acid (poly (I:C)), a synthetic double-stranded RNA analog [6, 7]. Together, these findings suggest that DUOX2 might also be involved in regulating the host defense against viral infection.

In this study, we show that *DUOX2* is a late antiviral gene induced by an autocrine/paracrine pathway specifically triggered in AECs by the synergistic action of two major cytokines, IFNβ and TNFα secreted upon Sendai virus (SeV) infection, a model of *Paramyxoviridae* viruses. We further unveil that the combination of IFNβ and TNFα acts through a novel, non-canonical signaling pathway dependent on STAT2 and IRF9, but entirely independent of STAT1. Functional analyses reveal that DUOX2-derived H_2O_2 is essential for AECs to mount an antiviral response specifically triggered by the synergism of IFNβ and TNFα. Importantly, we also reveal that respiratory syncytial virus (RSV), the most important etiological viral agent of pediatric respiratory tract diseases worldwide, has evolved mechanisms to counteract DUOX2 expression, allowing RSV to escape the DUOX2-mediated antiviral response. This observation highlights the importance of DUOX2 as a key molecule in the antiviral innate immune response.

Results

SeV infection induces DUOX2 and DUOXA2 expression in AECs

We previously reported that SeV infection of the A549 alveolar epithelial cell line induced DUOX2 mRNA expression, as demonstrated by RT-PCR [7]. Here, a detailed characterization of DUOX2 mRNA and protein expression following SeV infection was performed in different cell line models of AECs and non-transformed primary normal human bronchial epithelial cells (NHBEs). First, A549 cells were infected with SeV for various times. Quantitative RT-PCR (qRT-PCR) analyses revealed significant induction of DUOX2 mRNA levels starting at 24 h post infection (hpi) (Figure 1A, upper panel). Interestingly, induction of the classic early antiviral gene *interferon-induced protein with tetratricopeptide repeats 1* (*IFIT1*) started from 3 hpi and peaked between 6 hpi and 9 hpi (Figure 1A, lower panel). Thus, *DUOX2* belongs to a category of late virus-induced genes. DUOX2 induction was confirmed at the protein level by immunoblot analyses using anti-DUOX1/2 antibodies (Figure 1B). Although we and others previously reported that DUOX1 is not expressed in non-infected or SeV-infected A549 cells [7, 8], the specific detection of DUOX2 protein was confirmed by small interfering RNA (siRNA)-mediated knockdown of DUOX2 (Figures 3E, 5A and 6).

Functional expression of DUOX2 at the plasma membrane depends on the concomitant expression of its maturation factor DUOXA2 [9]. As *DUOX2* and *DUOXA2* genes are individually transcribed from the same bidirectional promoter [9], *DUOXA2* expression pattern likely resembles that of *DUOX2*. Indeed, DUOXA2 mRNA expression was induced in SeV-infected A549 cells, following kinetics similar to that of DUOX2 (Figure 1C). Infection of A549 cells with UV-treated SeV (SeV-UV) that is unable to replicate, failed to induce *DUOX2* expression, indicating that virus replication is essential for triggering the induction of *DUOX2* expression (Figure 1D). To further demonstrate that *DUOX2/DUOXA2* gene expression is responsive to SeV infection in AECs, we used polarized Calu-3 cells that were cultured at an air-liquid interface (ALI-Calu-3) and formed a tight monolayer. Calu-3 is a human serous gland cell line of sub-bronchial origin. ALI-Calu-3 are widely used in the studies of airway bar-
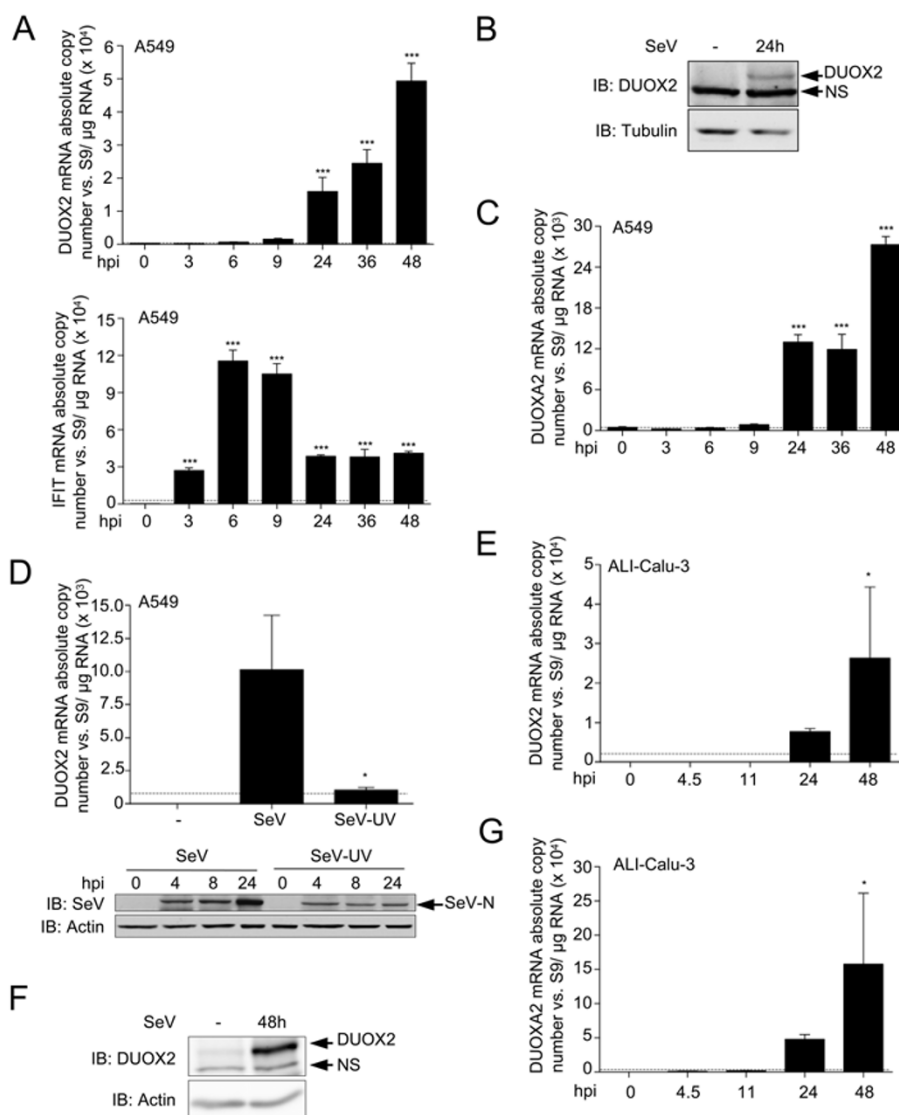
Figure 1 DUOX2 and DUOXA2 are induced upon SeV infection in AECs. **(A-C)** A549 cells were infected with SeV (40 HAU/10^6 cells) for the indicated times. **(D)** A549 cells were infected with SeV or UV-treated SeV (40 HAU/10^6 cells) for the indicated times. **(E-G)** Polarized Calu-3 cells cultured for 10 days in ALI (ALI-Calu-3) and presenting an UAR ≥ 800 Ω.cm² were infected with SeV (40 HAU/10^6 cells) at the apical side for the indicated times. In **A**, **C**, **D**, **E** and **G**, total RNA was extracted. DUOX2, IFIT1 or DUOXA2 mRNA absolute copy numbers were quantified by qRT-PCR. In **B** and **F**, DUOX2 protein expression was analyzed by immunoblot analyses using anti-DUOX1/2-specific antibodies. In **D**, SeV N protein expression was detected using anti-parainfluenza antibodies. Equal loading was verified using anti-tubulin or anti-actin antibody. All data are presented as mean ± SD. Statistical analyses were conducted using one-way ANOVA with Tukey post-test, except in **D**, where analysis was performed using a *t*-test. Statistical significances are presented compared with the non-infected control, except in **D**, where the SeV-infected condition is compared with SeV-UV-infected condition. $*P < 0.05$, $***P < 0.001$. The dotted line in qRT-PCR graphs represents the threshold of detection. IB, immunoblot; NS, non specific; hpi, hours post-infection; HAU, hemagglutinin units; UAR, unit area resistance.

rier function and ion secretion and were recently shown to be a suitable model for studying viral infections [10]. Monolayers of ALI-Calu-3 exhibiting good integrity, as determined by a transepithelial electric resistance (TEER) of ≥800 Ω.cm², were used in the experiments. Infection of ALI-Calu-3 with SeV on the apical side resulted in DUOX2 and DUOXA2 mRNA induction starting at 24 hpi (Figure 1E and 1G) and detectable DUOX2 protein levels at 48 hpi (Figure 1F). Importantly, DUOX2 and DUOXA2 mRNA induction was also confirmed in pri-

mary NHBEs infected with SeV for 24 h (Figure 7A). Altogether, these results demonstrate that *DUOX2* and *DUOXA2* are late virus-induced genes in human AECs.

SeV-induced DUOX2/DUOXA2 expression results from an autocrine/paracrine mechanism

The delayed induction of *DUOX2* and *DUOXA2* expression during SeV infection suggests that their expression might require *de-novo* protein synthesis and/or secretion of regulatory factor(s). To test this hypothesis, we harvested the supernatants of SeV-infected A549 cells (SN-SeV). The supernatants were then treated with UV irradiation (SN-SeV-UV) to impair the replication capacity of newly secreted virions, and consequently these virions should no longer be able to induce *DUOX2* expression (as shown in Figure 1D). Stimulation of fresh A549 cells with SN-SeV-UV (Figure 2A) still led to induction of DUOX2 and DUOXA2 mRNA to levels corresponding to $64 \pm 12\%$ and $88 \pm 33\%$, respectively, of those induced by the direct SeV infection (Figure 2B and 2D). Treatment with SN-SeV-UV also efficiently up-regulated DUOX2 protein expression (Figure 2C). Heat inactivation of SN-SeV-UV abolished DUOX2 mRNA and protein induction (Figure 2E). These results suggest that protein factors released into the supernatants of infected cells play a major role in the induction of *DUOX2/DUOXA2* expression. Next, the possibility that apoptosis of infected cells could contribute to the release of these factors was ruled out. The cells were infected with SeV in the presence of the pan-caspase inhibitor Z-VAD-FMK to block apoptosis as demonstrated by the efficient inhibition of PARP cleavage (Figure 2F). However, blockade of apoptosis failed to interfere with the capacity of the resulting SN-SeV-UV to induce DUOX2 mRNA expression (Figure 2F), demonstrating that *DUOX2* induction does not result from caspase-dependent apoptotic processes triggered by SeV infection. Altogether, these results highlight for the first time that *DUOX2/DUOXA2* induction in virus-infected AECs results from an autocrine/paracrine mechanism.

IFNβ and TNFα synergize to induce DUOX2 and DUOXA2 expression

Next, we sought to determine the identity of the soluble factor(s) responsible for SeV-stimulated induction of *DUOX2/DUOXA2*. Although type I (α and β) and type III (λ1-3, also known as IL28/IL29) IFNs are the most abundant cytokines secreted following viral infection, stimulation of A549 cells with recombinant IFNβ (Figure 3A and 3B) or IFNα2b, IL28 or IL29 (data not shown) failed to induce significant increase in DUOX2 or DUOXA2 mRNA levels. Interestingly, previous re-

ports revealed that IFNβ can synergize with TNFα to induce a late antiviral state distinct from the early state induced by IFNβ alone [11, 12]. Thus, we tested the possibility that *DUOX2/DUOXA2* induction could be driven by the combination of IFNβ and TNFα. Multiplex ELISA analyses confirmed the presence of both IFNβ and TNFα in the SN-SeV derived from A549 cells (Figure 3C). Interestingly, stimulation of A549 cells with a combination of recombinant IFNβ and TNFα led to a significant increase in DUOX2 and DUOXA2 mRNA and DUOX2 protein levels as compared with stimulation with either cytokine individually (Figure 3A and 3B). Similar results were observed in primary NHBEs (Figure 7B). Several other combinations of IFNα, IFNβ or TNFα with IFNλ (IL28/IL29) were tested, but none of them resulted in DUOX2 induction (Supplementary information, Figure S1). To demonstrate the importance of IFNβ and TNFα in the capacity of SN-SeV-UV to induce *DUOX2/DUOXA2* expression, siRNA was used to knock down type I IFN receptor chain 1, IFNAR1, and TNFα receptor, TNFRSF1A. Depletion of either of the receptors led to decreased DUOX2 mRNA induction following SN-SeV-UV treatment as compared with control cells (Figure 3D). Importantly, the combination of IFNβ and TNFα, similar to SeV infection, induced catalase-sensitive H_2O_2 production (Figure 3E). The H_2O_2 induction was also dramatically reduced by DUOX2 silencing using a specific siRNA, demonstrating that DUOX2 is a main source for and IFNβ- and TNFα-stimulated H_2O_2 generation (Figure 3E). Altogether, these results unveil the synergistic action of IFNβ and TNFα in the autocrine/paracrine regulation of *DUOX2/DUOXA2* expression during viral infection.

DUOX2 induction is mediated by a non-canonical, STAT2/IRF9-dependent, but STAT1-independent pathway

To further identify the mechanisms involved in virus-triggered induction of *DUOX2* expression, an RNAi strategy was pursued to individually knock down each subunit of the ISGF3 complex, STAT1, STAT2 and IRF9. Surprisingly, while knockdown of STAT2 and IRF9 strongly diminished SN-SeV-UV-induced DUOX2 mRNA and protein expression compared with the control cells, STAT1 knockdown (mediated by siSTAT1(1)) did not impair *DUOX2* induction (Figure 4A). Similar results were obtained using another STAT1-specific siRNA (siSTAT1(2)) (Figure 4B). Although siSTAT1(1) led to an increase of DUOX2 mRNA expression (Figure 4A), this increase was not reproduced with siSTAT1(2) (Figure 4B), and the effect was therefore not considered specific. By contrast, both STAT1-specific siRNAs efficiently inhibited IFNγ-induced interferon regulatory factor (IRF1) expression (Figure 4C).
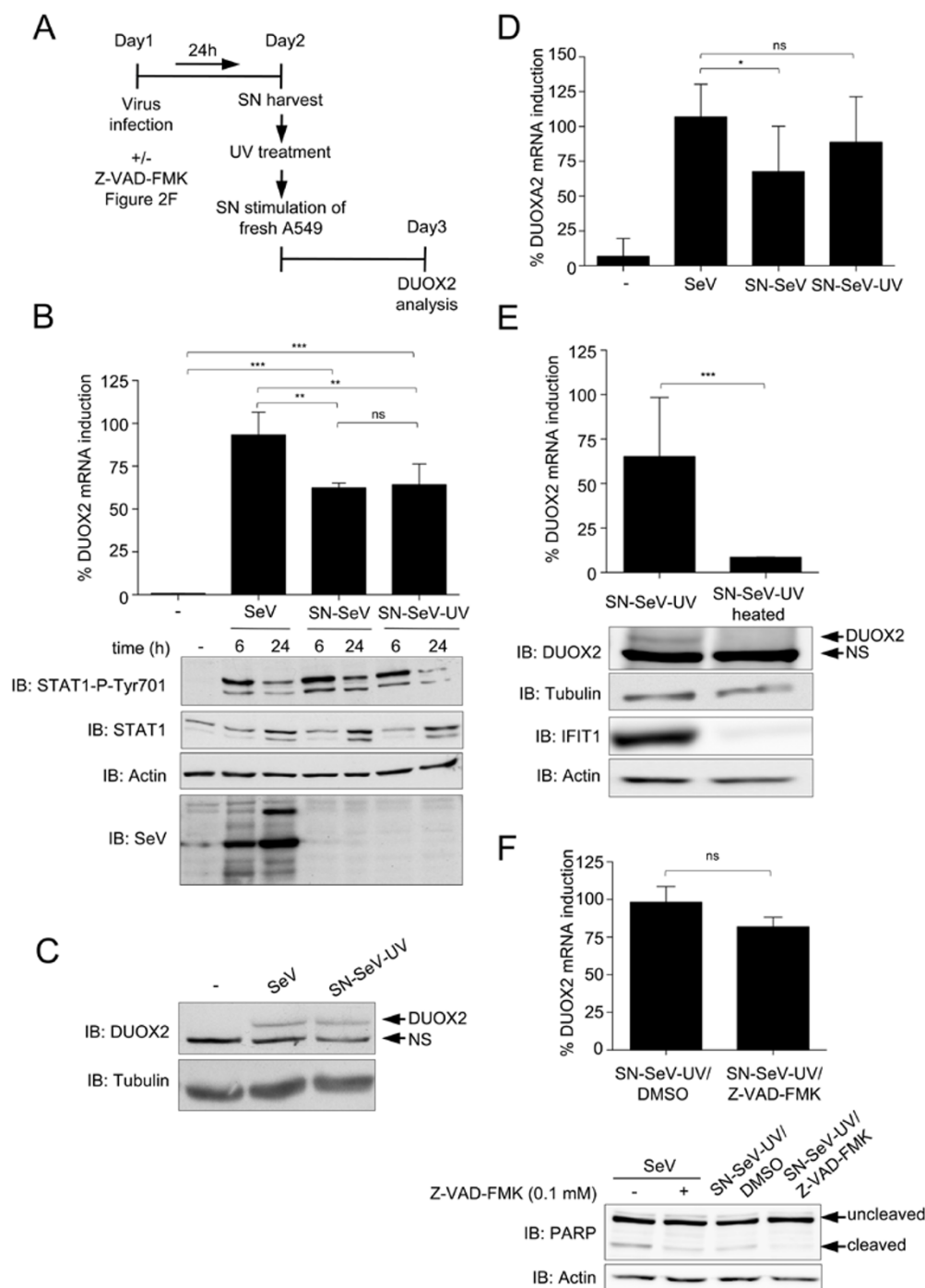
Figure 2 SeV induces DUOX2 and DUOXA2 expression through secreted proteins. **(A)** A schematic outline of the timeline used for experiments in **B**-**F**. **(B**-**D)** A549 cells were stimulated with untreated (SN-SeV) or UV-treated supernatants (SN-SeV-UV) from SeV-infected (40 HAU/10^6 cells) for 24 h **(C**, **D)** or the indicated times **(B)**. SeV infection (40 HAU/10^6 cells, 24 h) was conducted as comparison. **(E)** A549 cells were stimulated with SN-SeV-UV or SN-SeV-UV subjected to heat treatment. In **B**, **D** and **E**, DUOX2 or DUOXA2 mRNA expression was analyzed by qRT-PCR. In **B**, **C**, and **E**, immunoblot analyses were performed to measure the protein expression levels of phosphorylated STAT1 (STAT1-P-Tyr701), STAT1, SeV, DUOX2 or IFIT1. **(F)** A549 cells were treated for 24 h with SN-SeV-UV generated from cells exposed to DMSO (SN-SeV-UV/DMSO) or 0.1 mM Z-VAD-FMK (SN-SeV-UV/Z-VAD-FMK). DUOX2 mRNA expression was analyzed by qRT-PCR. PARP cleavage was assessed in SeV-infected A549 cells treated with DMSO or Z-VAD-FMK, as well as in cells stimulated with SN-SeV-UV/DMSO or SN-SeV-UV/Z-VAD-FMK. qRT-PCR data are presented as mean ± SD. Statistical analysis was conducted using one-way ANOVA with Dunnett post-test, except in **E** and **F**, where a *t*-test was used. *$P < 0.05$, **$P < 0.01$, ***$P < 0.001$.
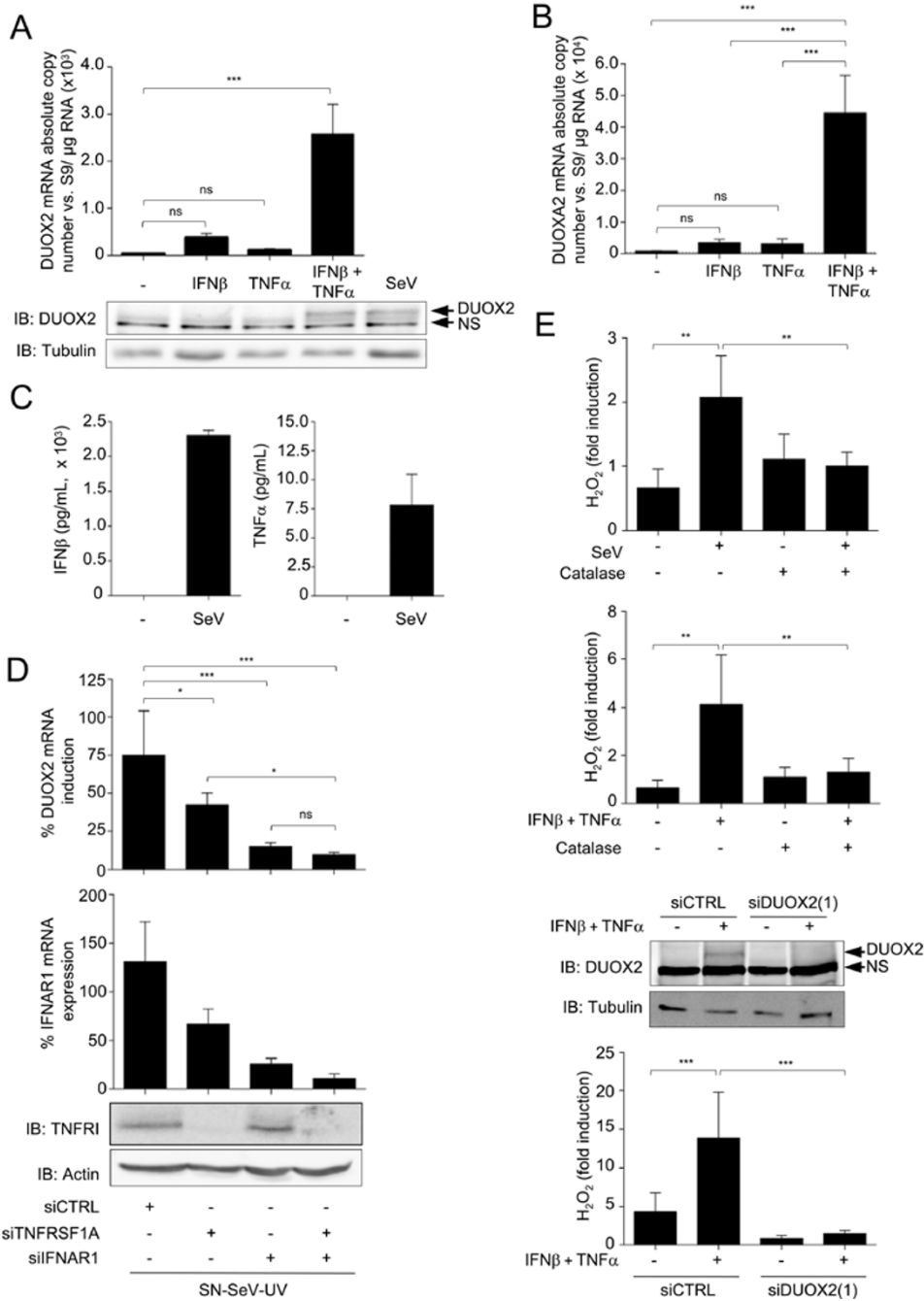
Figure 3 Costimulation by IFNβ and TNFα efficiently induces DUOX2 and DUOXA2 expression and DUOX2-dependent H_2O_2 production. **(A, B)** A549 cells were stimulated with recombinant IFNβ and/or TNFα for 24 h. SeV infection (40 HAU/10^6 cells, 24 h) was conducted for comparison. DUOX2 or DUOXA2 mRNA absolute copy numbers were analyzed by qRT-PCR. In **A**, DUOX2 protein expression was analyzed by immunoblot analyses. **(C)** A549 cells were infected with SeV (40 HAU/10^6 cells). IFNβ and TNFα levels in the supernatants were measured by Multiplex ELISA. **(D)** A549 cells were transfected with control siRNA (siCTRL) or siRNA targeting IFNAR1 using a mixture of siIFNAR1(1) and siIFNAR1(2), and/or siRNA targeting TNFRSF1A using siTNFRSF1A. Forty-eight hours post-transfection, cells were stimulated with SN-SeV-UV for 24 h. IFNAR1 expression levels were analyzed by qRT-PCR and TNFRI levels were detected by immunoblot analyses. **(E)** A549 cells were stimulated as in **A**. Where indicated, the cells were transfected with siCTRL or siRNA targeting DUOX2 (siDUOX2(1)) 48 h prior to stimulation. H_2O_2 production was analyzed using the HVA assay. Where indicated, catalase was added at 400 U/ml. All qRT-PCR and H_2O_2 measurement data are presented as mean ± SD. Fold induction is calculated over the corresponding non-stimulated condition. The pointed line in graphs represents the threshold of detection. Statistical analysis was conducted by one-way ANOVA using Tukey multiple comparison analysis. *$P < 0.05$, **$P < 0.01$, ***$P < 0.001$.
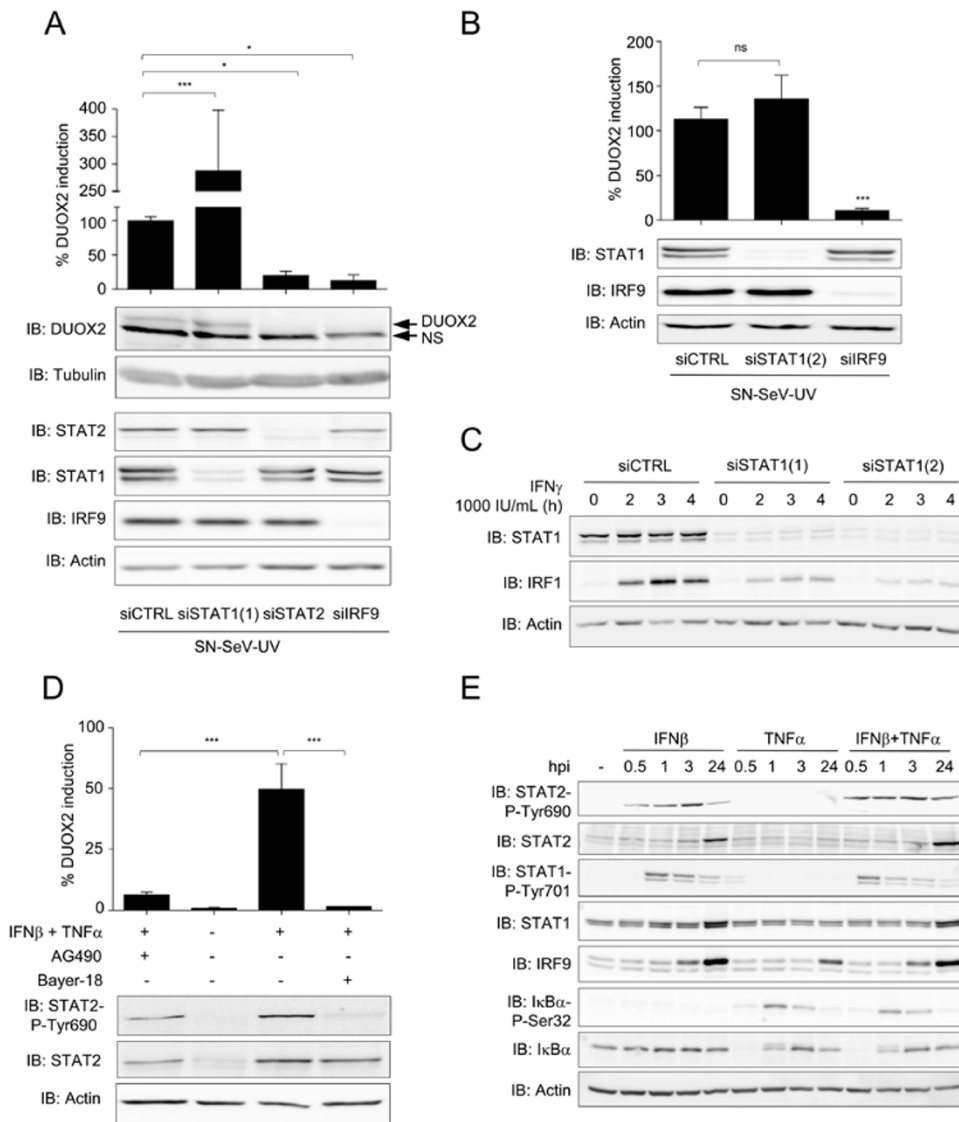
Figure 4 DUOX2 induction is regulated in a STAT2/IRF9-dependent, STAT1-independent manner. **(A-C)** A549 cells were transfected with siRNA specific for STAT1, STAT2 or IRF9. Forty eight h post-transfection, cells were stimulated with SN-SeV-UV for 24 h in **A** and **B** or IFNγ for the indicated time in **C**. **(D)** A549 cells were pretreated with AG490 (100 μM), Bayer-18 (100 μM) or DMSO (vehicle) for 1 h before stimulation with IFNβ and TNFα for 24 h. In **A**, **B** and **D**, DUOX2 mRNA absolute copy number was analyzed by qRT-PCR and DUOX2 levels were expressed as % of the siCTRL condition (**A**, **B**) or as % of the control cells **(D)**. In **A-E,** DUOX2, STAT2-P-Tyr690, STAT2, STAT1-P-Tyr701, STAT1, IκBα-P-Ser32, IκBα, or IRF9 protein levels were analyzed by immunoblot. All qRT-PCR data are presented as mean ± SD. Data were analyzed by one-way ANOVA with Dunnett post-test. *$P < 0.05$, *** $P < 0.001$.

In the ISGF3 complex, activated STAT2 is phosphorylated on Tyr690. To evaluate whether STAT2-Tyr690 phosphorylation is also required in the non-canonical pathway leading to DUOX2 induction, the JAK kinases inhibitor, AG490, and the specific inhibitor of the JAK kinase Tyk2, Bayer-18, were used. Both inhibitors efficiently inhibited STAT2-Tyr690 phosphorylation and dramatically reduced DUOX2 induction in IFNβ- and

TNFα-stimulated cells (Figure 4D). Interestingly, kinetic analysis of STAT2 phosphorylation in response to IFNβ and/or TNFα, revealed that although TNFα alone was not sufficient to trigger STAT2 phosphorylation, it helped to enhance IFNβ-induced STAT2 phosphorylation during an extended period of time. Additionally, TNFα alone was able to increase IRF9 expression (Figure 4E). The impacts of TNFα on IRF9 expression and on STAT2

phosphorylation most likely contribute to the activation of the non-canonical STAT2/IRF9 pathway during co-stimulation by IFNβ and TNFα. TNFα is well known to trigger NF-κB-dependent gene expression. However, no significant differences were observed in IκBα phosphorylation and degradation between TNFα-stimulated- and IFNβ/TNFα-costimulated cells (Figure 4E). Additionally, ectopic expression of the widely used super-repressor of NF-κB pathway, IκBα2NΔ4 [13], did not prevent SN-SeV-UV-induced DUOX2 expression (Supplementary Figure S3), strongly suggesting that NF-κB is unlikely to be involved in IFNβ- and TNFα-mediated induction of DUOX2. Hence, a non-canonical signaling pathway involving IRF9 and phosphorylated STAT2, but not STAT1, mediates the IFNβ- and TNFα-dependent induction of DUOX2 in AECs during SeV infection.

DUOX2 is essential for AECs to mount an antiviral defense

It has not yet been assessed whether *DUOX2* is one of the numerous virus-induced genes that allow the host to mount an antiviral response. To evaluate the antiviral role of DUOX2, SN-SeV-UV generated from A549 cells or a combination of IFNβ and TNFα were used to stimulate A549 cells transfected with control siRNA (siCTRL) or two different DUOX2-specific siRNAs (siDUOX2(1) and siDUOX2(2)). The antiviral responses of the target cells were then monitored through their capacity to limit the replication of a recombinant RSV encoding GFP (RecRSV-GFP) (Figure 5A). As shown in Figure 5B, siCTRL-transfected, SN-SeV-UV-treated cells efficiently restricted RecRSV-GFP replication as compared with siCTRL-transfected cells. Importantly, in the absence of DUOX2, SN-SeV-UV-treated cells were less effective in restricting RecRSV-GFP replication as compared with siCTRL-transfected, SN-SeV-UV-treated cells. Thus, in the absence of DUOX2, cells mount a less-efficient antiviral response following stimulation with SN-SeV-UV. Similar results were obtained in the context of IFNβ and TNFα costimulation (Figure 5C, upper panel). Importantly, DUOX2 siRNA did not alter the antiviral state induced by IFNβ alone (Figure 5C, lower panel) that failed to trigger DUOX2 expression (Figure 3A), highlighting the specific role of DUOX2 in the antiviral state mounted in response to IFNβ and TNFα costimulation. Additionally, the antiviral effect triggered by IFNβ and TNFα was inhibited by the treatment with catalase, thereby demonstrating that the antiviral state relies on H_2O_2 production (Figure 5D). The role of DUOX2 in the establishment of the IFNβ- and TNFα-dependent antiviral response was also confirmed in primary NHBEs (Figure 7B). Altogether, these results are the first to unveil the contribution of DUOX2 to the development of the antiviral state in AECs.

Next, to elucidate how DUOX2 enhances the antiviral state, multiplex ELISA analyses were performed to measure type I and type III IFN levels, the major antiviral cytokines secreted during viral infection of AECs, in the supernatants of A549 cells that were transfected with siCTRL or siDUOX2(1)/(2) and infected with SeV. Interestingly, absence of DUOX2 significantly diminishes IFNβ levels at 24 hpi and 32 hpi, and IFNλ levels at 32 hpi (Figure 6A). On the other hand, TNFα levels were not significantly changed (Figure 6A). Despite the observation that siDUOX2(1)-mediated DUOX2 knockdown diminished TNFα levels, although not significantly, the result was not confirmed using siDUOX2(2) (Figure 6A). Similar results were observed in primary NHBEs (Figure 7C). Importantly, none of the cytokine levels were significantly altered by DUOX2 knockdown at 6 hpi, thereby suggesting that DUOX2 controls the sustained levels of IFNβ and IFNλ specifically at late stages of viral infection. Importantly, the effects of DUOX2 depletion on levels of the cytokines could not be explained by the changes of their respective mRNA levels (Figure 6B). Thus, our results demonstrate that DUOX2 is a key factor in the establishment of an antiviral state triggered by the synergism between IFNβ and TNFα, and that it acts at least in part through the regulation of IFNβ and IFNλ protein levels at late time points of infection.

RSV interferes with the expression of DUOX2

The aforementioned data clearly highlight a new antiviral pathway occurring in the airway epithelium, which is mediated by the synergism between IFNβ and TNFα involving the induction of DUOX2. Key antiviral pathways are often targeted by evasion mechanisms evolved by pathogenic viruses, including RSV [14]. Thus, we next sought to determine whether RSV is capable of evading the DUOX2-dependent antiviral response. First, A549 cells were infected with RSV for various periods. As shown in Figure 8A, RSV infection induced only weak levels of DUOX2 mRNA compared with SeV infection. RSV infection failed to induce detectable levels of the DUOX2 protein, even when the multiplicity of infection (MOI) was increased from 3 to 10 (Figure 8B). Analysis of DUOXA2 mRNA levels again revealed a barely detectable induction during RSV infection, which was significantly lower than the one observed during SeV infection (Figure 8C). Similar results were observed in the ALI-Calu-3 model (Figure 8D-8F). Importantly, IFNβ and TNFα levels in the supernatant of RSV-infected A549 cells were close to those detected in the supernatant of SeV-infected A549 cells (Figure 8G vs
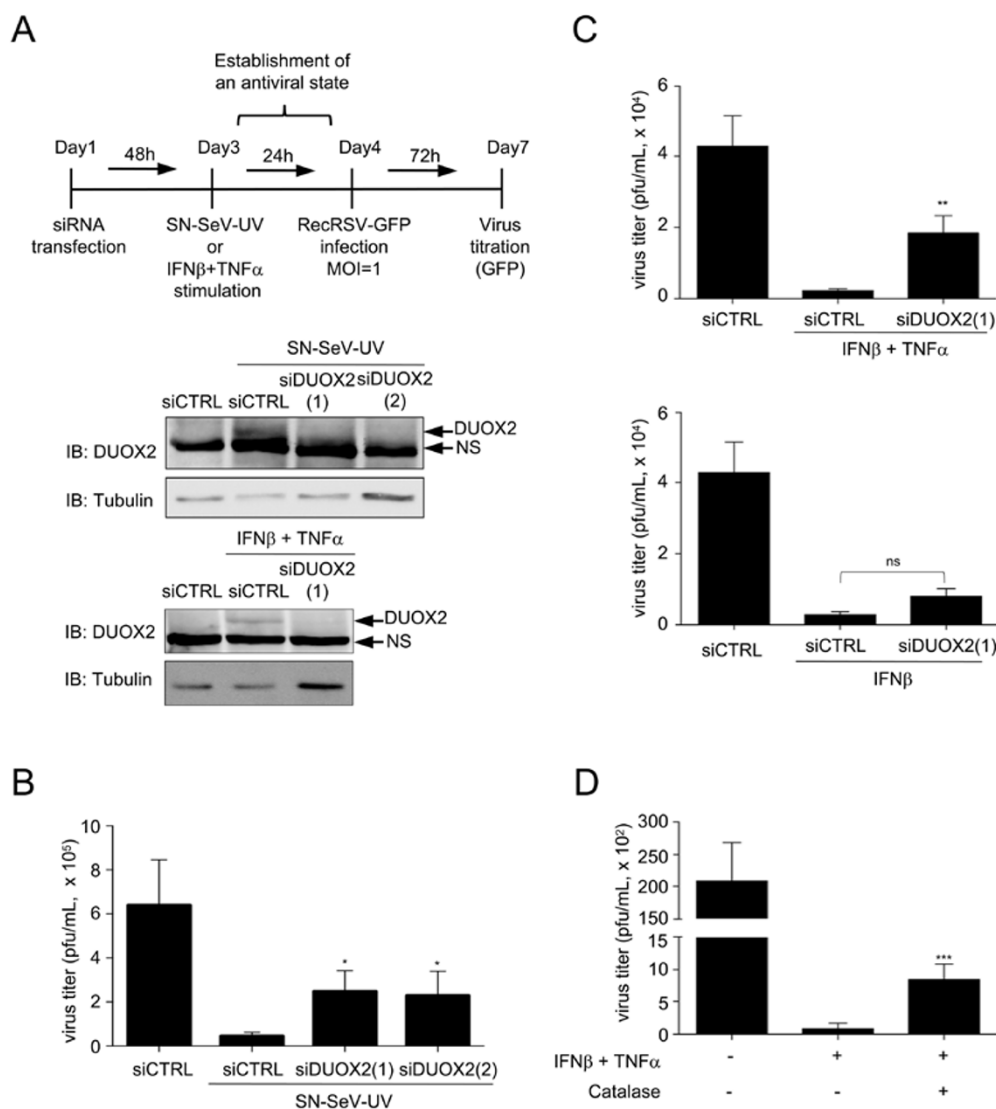
Figure 5 DUOX2 is necessary for the establishment of an H_2O_2-dependent antiviral state. **(A)** A schematic outline of the experimental timeline used for experiments in **B**-**D**. **(B-D)** A549 cells were transfected with siCTRL, siDUOX2(1) or siDUOX2(2) before being stimulated with SN-SeV-UV or with IFNβ and TNFα for 24 h. DUOX2 expression was analyzed by immunoblot analyses using DUOX1/2 antibody. Twenty-four h post-stimulation with SN-SeV-UV or cytokines, cells were infected with recombinant RecRSV-GFP at a MOI of 1 for 72 h and the release of infectious viral particles was quantified by plaque forming unit assay. Catalase was added 6 h prior to RecRSV-GFP infection in **D**. All data are presented as mean ± SD. Data were analyzed by one-way ANOVA with Dunnett post-test, siCTRL vs siDUOX2(1) or siDUOX2(2) in **B** and **C**, or IFNβ + TNFα vs IFNβ + TNFα + catalase in **D**. *$P < 0.05$, **$P < 0.01$, ***$P < 0.001$.

Figure 3C). Hence, the decreased *DUOX2* and *DUOXA2* induction during RSV infection could not be attributed to a deficiency in the production of IFNβ or TNFα. Interestingly, UV-treated supernatants derived from RSV-infected A549 cells (SN-RSV-UV), when used as in Figure 2A, induced DUOX2 mRNA expression to levels corresponding to 305 ± 125% of those induced by direct RSV infection (Figure 8H) and detectable levels of DUOX2 protein (Figure 8I). Similar to our observation in the context of

SeV infection, knockdown of STAT2 and IRF9, but not of STAT1, prior to SN-RSV-UV stimulation, impaired DUOX2 induction (Figure 8J). Altogether, these results demonstrate that cytokines secreted in response to RSV infection are capable of inducing *DUOX2* expression, but the presence of the virus in the cells interferes with *DUOX2* induction, allowing RSV to escape the DUOX2-mediated antiviral response.
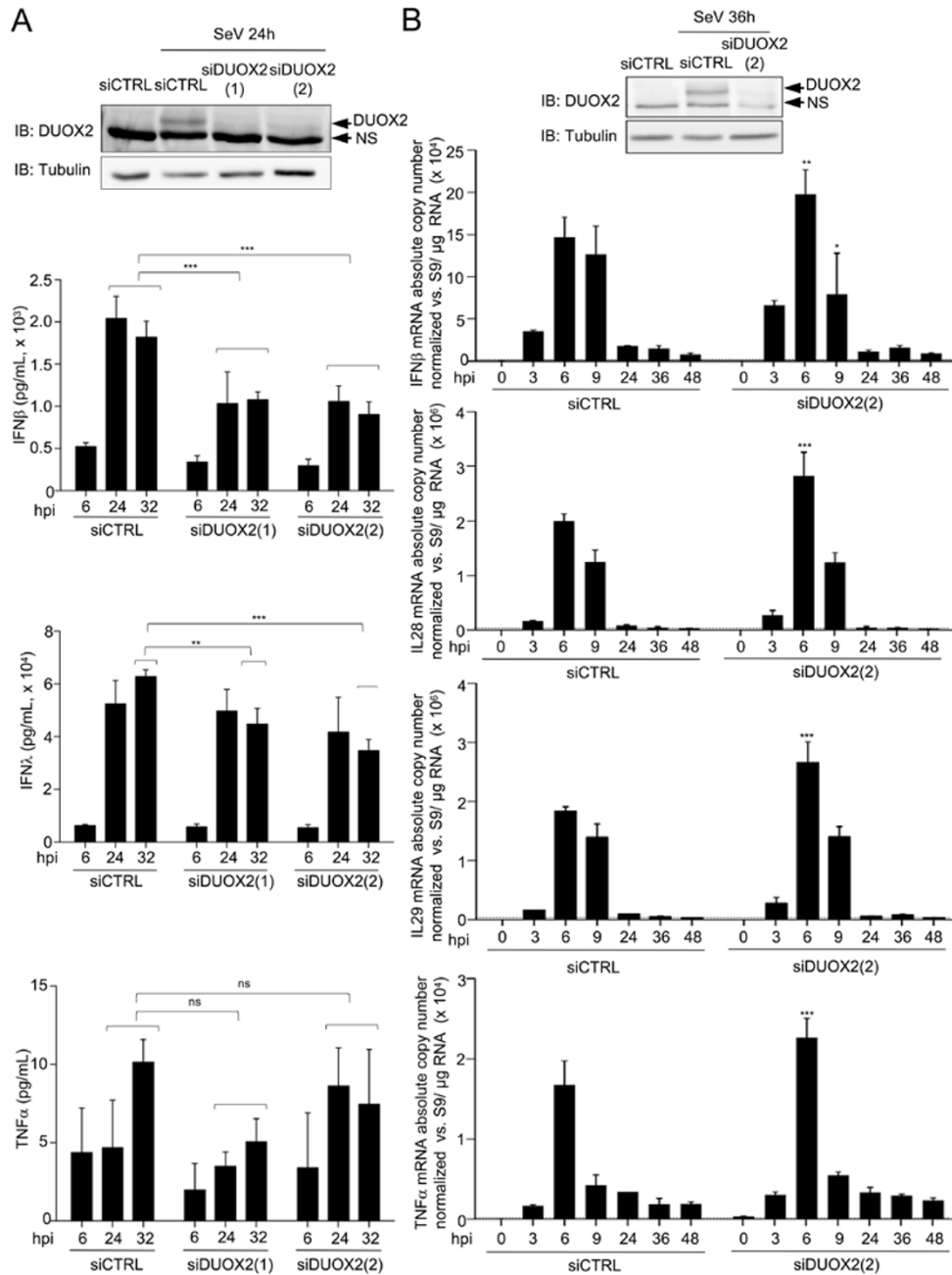
Figure 6 DUOX2 regulates secreted levels of type I/III IFNs at the late stages of viral infection. **(A)** A549 cells were transfected with siCTRL, siDUOX2(1) or siDUOX2(2), and 48 h post-transfection, cells were infected with SeV (40 HAU/10⁶ cells) for the indicated times. DUOX2 expression was analyzed by immunoblot analyses using DUOX1/2 specific antibodies. Release of IFNβ, IFNλ and TNFα was measured by multiplex ELISA. **(B)** A549 cells were transfected with siCTRL or siDUOX2(2) for 48 h and infected as in **A** for the indicated times. IFNβ, IFNλ (IL-28A and IL-29) and TNFα mRNA absolute copy numbers were analyzed by qRT-PCR. Data were analyzed by two-way ANOVA with Bonferroni post-test. $*P < 0.05$, $**P < 0.01$, $***P < 0.001$. The dotted line in qRT-PCR graphs represents the threshold of detection.

Discussion

AECs are the first line of defense against respiratory virus infection. The efficiency of the innate antiviral state mounted by AECs critically influences the outcome of viral infection. In the current paradigm, the antiviral state
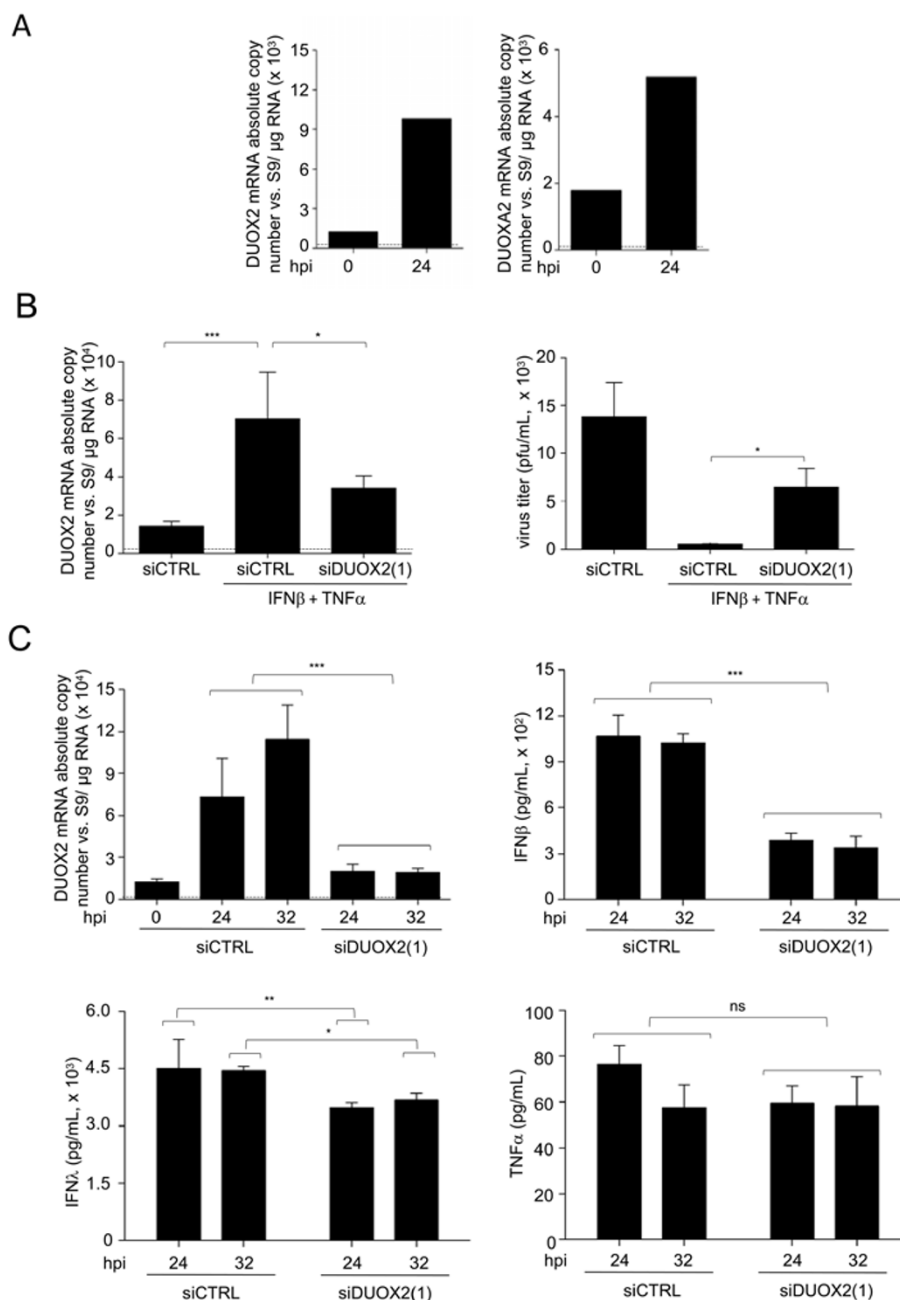
Figure 7 DUOX2 induction controls a late IFNβ/TNFα-dependent antiviral state in NHBEs. **(A)** NHBEs were infected with SeV (40 HAU/10^6 cells) for 24 h. DUOX2 or DUOXA2 expression levels were analyzed by qRT-PCR. **(B**, **C)** NHBEs were transfected with siCTRL or siDUOX2(1) and then stimulated with IFNβ and TNFα for 24h before RecRSV-GFP infection **(B)**, or infected with SeV for the indicated times **(C)**. DUOX2 expression levels were analyzed by qRT-PCR. In **B**, infectious virion release was quantified as described in Figure 5. In **C**, release of IFNβ, IFNλ and TNFα was measured by multiplex ELISA. Data were analyzed by one-way ANOVA with Dunnett post-test in **B**. Data were analyzed by two-way ANOVA with Bonferroni post-test in **C**. *$P < 0.05$, **$P < 0.01$, ***$P < 0.001$. The dotted line in qRT-PCR graphs represents the threshold of detection.

in infected AECs is primarily dependent on type I IFNs-mediated activation of the JAK/STAT signaling cascade that ultimately leads to the transcriptional control of ISGs by the ISGF3 complex. Here, we highlight a novel antiviral pathway occurring in AECs, which is initiated by the synergistic autocrine/paracrine action of IFNβ and TNFα, and signals through an IRF9- and STAT2-dependent, but entirely STAT1-independent, non-canonical cascade to
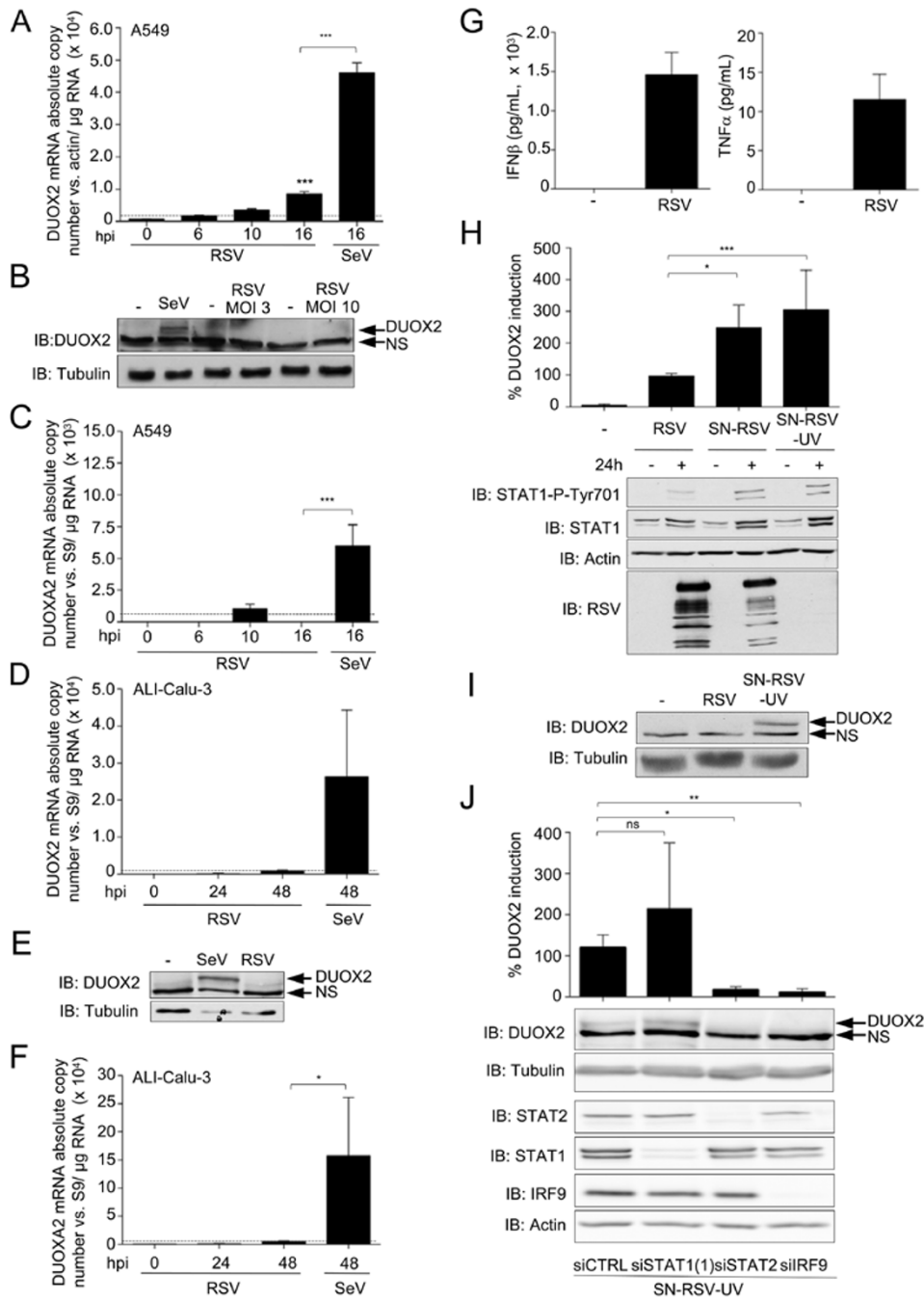
Figure 8 SN-RSV-UV triggers higher expression of DUOX2 than direct RSV infection. **(A, C)** A549 cells were infected with RSV at an MOI of 3 for the indicated times. SeV infection (40 HAU/10^6 cells) was conducted for comparison. **(B)** A549 cells were infected with RSV at an MOI of 3 or 10 or with SeV at 40 HAU/10^6 cells for 24 h. **(D-F)** ALI-Calu-3 cells were infected with RSV at an MOI of 3 for the indicated times, or for 24h in **E**. **(G)** A549 cells were infected with RSV at an MOI of 3 for 24 h. IFNβ/TNFα levels in the supernatants were measured by multiplex ELISA. **(H, I)** A549 cells were stimulated with SN-RSV or UV-treated supernatants (SN-RSV-UV) for 24 h. RSV infection (MOI = 3, 24 h) was conducted for comparison. **(J)** A549 cells were transfected with siRNAs as in Figure 4A, and 48 h post-transfection, cells were stimulated with SN-RSV-UV for 24 h. In **A**, **C**, **D**, **F**, **H**, and **J**, DUOX2 or DUOXA2 mRNA levels were quantified by qRT-PCR. These values are presented as % DUOX2 induction in **H** and **J**. In **B**, **E**, **H**, **I** and **J**, immunoblot analyses were performed to analyze the protein expression of DUOX2, STAT1-P-Tyr701, STAT1, RSV, STAT2 or IRF9. All qRT-PCR data are presented as mean ± SD. Data were analyzed by one-way ANOVA with Tukey post-test except in **J**, where a Dunnett post-test was used; $*P < 0.05$, $**P < 0.01$, $***P < 0.001$. The pointed line in qRT-PCR quantification data represents the threshold of detection.
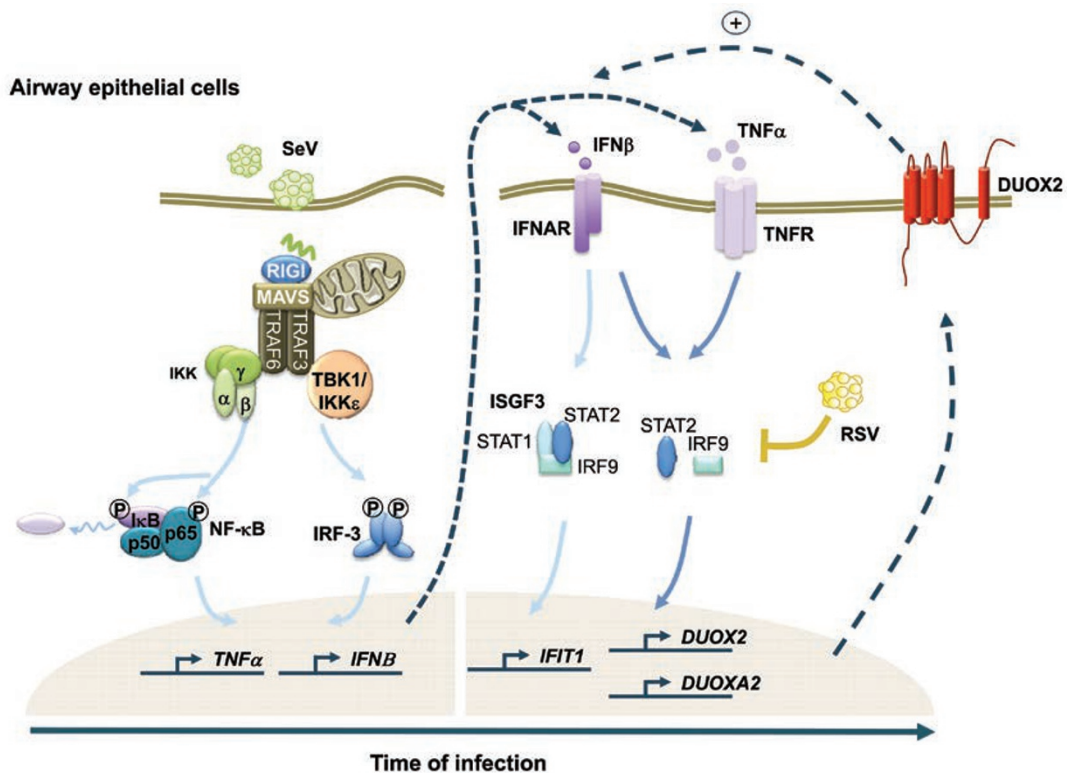
Figure 9 Model of the innate immune antiviral response triggered by IFNβ and TNFα in AECs. SeV infection of AECs triggers the secretion of IFNβ and TNFα. Binding of IFNβ to its cognate receptor activates the "classic" antiviral pathway mediated by the ISGF3 TF. Additionally, the synergism between IFNβ and TNFα induces late DUOX2 expression through a non-canonical antiviral signaling pathway. This pathway involves STAT2 and IRF9, but is entirely independent of STAT1. Late DUOX2 induction and H_2O_2 production is essential for the cells to mount an efficient antiviral state, at least in part through the regulation of IFNβ and IFNλ levels at late time points of infection. The importance of this novel airway antiviral defense mechanism is underlined by the observation that pathogenic RSV is able to counteract DUOX2 induction, suggesting that RSV has evolved a strategy to evade the DUOX2-dependent antiviral response.

establish a late antiviral state mainly controlled by the DUOX2 NADPH oxidase (Figure 9).

Virus infections trigger the secretion of multiple antiviral and proinflammatory cytokines that bind to their cognate receptors to engage specific signaling pathways. Although it seems intuitive that secreted cytokines do not act independently, but rather simultaneously to foster the antiviral response, the specific outcomes resulting from their cooperation have barely been described. The synergism between IFNβ and TNFα was first reported in 1988 [15]. However, it was only recently discovered, through microarray profiling, that IFNβ and TNFα synergize to drive the expression of a panel of late genes that define a distinct antiviral state. These genes are not responsive to IFNβ or TNFα alone, or they are only responsive to one of the cytokines when used separately [11, 12]. Here, we uncover that in AECs, *DUOX2* and *DUOXA2* belong to this category of late genes that are not significantly induced by IFNβ or TNFα alone, but are remarkably

induced to high levels in response to the combination of IFNβ and TNFα. Previous attempts to identify the mechanisms underlying the specific regulation of genes dependent on IFNβ and TNFα synergism were performed through bioinformatic analyses of the promoters of this panel of genes in order to identify enrichment of specific transcription factor (TF)-binding sites. However, no specific TF was identified [11]. Here, through a targeted strategy using siRNA, we demonstrate for the first time that the synergistic action of IFNβ and TNFα engages a specific STAT2- and IRF9-dependent, but STAT1-independent, signaling pathway. Interestingly, our results reveal that TNFα contributes to IRF9 induction and that TNFα synergism with IFNβ induces an enhanced and sustained activation of JAK-mediated STAT2 phosphorylation. Thus, IRF9 induction and STAT2 phosphorylation likely contribute to the activation of the non-canonical STAT2/IRF9 pathway during costimulation by IFNβ/TNFα. This is consistent with previous reports that TNFα

mediates the activation of JAKs [16, 17]. It remains to be determined whether this STAT2- and IRF9-dependent pathway is responsible for the regulation of all the other genes previously identified to be responsive to the combination of IFNβ and TNFα. Other studies have proposed that TNFα synergizes with IFNβ through an autocrine/paracrine loop. Indeed, TNFα can induce the secretion of IFNβ in an IRF1-dependent manner, thereby controlling the expression of specific late genes through the classic JAK/STAT pathway [12, 18, 19]. However, this loop is unlikely to be involved in the induction of DUOX2 in our system, as TNFα alone is not sufficient to activate *DUOX2/DUOXA2* expression.

Previous reports have described the capacity of STAT2 and IRF9 to activate gene transcription independently of STAT1 [20-24]. However, none of these studies have linked the activation of the STAT2/IRF9 pathway to the specific synergistic action of IFNβ and TNFα. Interestingly, in the absence of STAT1, STAT2/IRF9 display only limited DNA-binding affinity to the typical interferon-sensitive response element (ISRE) targeted by the IRF9 DNA-binding domain [20], and the consensus DNA-binding sequence for this non-canonical complex remains to be determined. The possibility that the STAT2/IRF9 complex binds to a yet uncharacterized consensus-responsive element would explain the failure of the previous bioinformatic strategy aimed at identifying TFs acting downstream of IFNβ and TNFα, as it was based on the databases of known DNA-binding consensus sites [11]. It is noteworthy to mention that all-trans retinoic acid (ATRA) was reported to stimulate the STAT2/IRF9-dependent induction of *RIG-G* gene expression [25]. Interestingly, ATRA was shown to be a potent inducer of *DUOX2* in AECs [26].

To date, the regulation of *DUOX2/DUOXA2* expression has been mainly investigated in thyrocytes, as well as in airways and gut epithelial cells following bacterial infection [6, 27-29]. Our observation that *DUOX2/DUOXA2* were induced following SeV infection in three different AEC models, A549, ALI-Calu-3 and NHBEs, adds to the picture of the previously reported RV-induced *DUOX2/DUOXA2* expression in primary AECs [6, 30-32]. Importantly, SeV is a member of the *Paramyxoviridae* family of negative sense single-stranded RNA (ssRNA) viruses, whereas RV belongs to the *Picornaviridae* family containing positive sense ssRNA viruses. Furthermore, poly (I:C) used to engage TLR3 also induces DUOX2 expression in primary AECs [6]. Altogether, these data strongly support the idea that the DUOX2-dependent antiviral pathway might be relevant to a broad number of respiratory viruses. Interestingly, infection by RSV barely triggered detectable induction of *DUOX2/*

DUOXA2 expression. In contrary, SN-RSV-UV was a potent inducer of *DUOX2/DUOXA2*, thus suggesting that the presence of replicating RSV interferes with *DUOX2/DUOXA2* induction. This is of particular significance, as most human pathogenic viruses have evolved strategies to circumvent the key mechanisms of the innate antiviral response for their own replication needs [14]. Thus, the observation that *DUOX2/DUOXA2* expression is the target for viral evasion points to the importance of DUOX2 in the capacity of the host to mount an efficient antiviral response. In this line, we unveil for the first time that DUOX2 is critical for the outcome of respiratory virus infections through its key function in the establishment of the antiviral state specifically induced by the synergistic action of IFNβ and TNFα secreted during SeV infection. The capacity of RSV to counteract this novel antiviral pathway adds to its previously recognized capacity to interfere with other key antiviral events, including RIG-I-dependent signaling or IKKε, TRAF3 or STAT2 stability [33, 34]. Altogether, these evasion mechanisms contribute to the development of RSV-associated diseases. Interestingly, DUOX2 expression is decreased in patients with cystic fibrosis (CF) [35]. Thus, our data shed lights on a potential mechanism for the increased susceptibility of CF patients to respiratory virus infections [36].

Up to date, the demonstration of a role of DUOX2 in the antimicrobial defense has been restricted to bacterial infections. This function of DUOX2 appears to be evolutionarily conserved. In *Drosophila*, absence of the DUOX homologue at epithelial surfaces profoundly alters the outcome of intestinal bacterial infection and fly survival [37]. At airway surfaces, H_2O_2 in combination with the secreted lactoperoxidase (LPO) enzyme and thiocyanite forms the microbicidal compound hypothiocyanate. To date, studies based on the use of antioxidant enzymes support the necessity of H_2O_2 in the LPO-dependent antibacterial defense [38]. Further studies suggest that DUOX2 is a source of H_2O_2 production in the airways [39, 40]. However, none of these studies have clearly demonstrated a functional connection between DUOX2-mediated H_2O_2 production and LPO-dependent airway antibacterial defenses. Whether the H_2O_2/LPO system contributes to the antiviral defense still remains to be clarified. *In vitro* studies have shown that the products of LPO activity, hypothiocyanate and hypoiodous acid, possess virucidal properties [41-43]. However, no data are available showing this activity in an *in vivo* context. In our setting, the H_2O_2/LPO system is unlikely to have a role based on the following observations. First, LPO is not secreted from *in vitro* cultured AECs [44] and all the studies that previously demonstrated an LPO-dependent antimicrobial function required the addition of LPO in

the experiments [38, 39, 43]. However, here we observe an antiviral effect of DUOX2 without the ectopic addition of LPO. Moreover, we do not observe an antiviral effect of the supernatant in a cell-free system (Supplementary information, Figure S2). Rather than a role in the synthesis of extracellular virucidal components, we identify a significant role of DUOX2 in the regulation of secreted levels of IFNβ and IFNλ, but not of TNFα (Figure 6A), nor IFNα, IFNω, IFNγ, IL6, or IL1α (data not shown). Interestingly, DUOX2 specifically regulates IFNβ and IFNλ levels at late time points of infection (starting at 24 hpi and 32 hpi, respectively), but not at the early time point (6 hpi). Hence, DUOX2 seems to play a role in sustaining the levels of IFNβ and IFNλ during viral infection. Further studies will be required to unveil how DUOX2 fosters sustained IFNβ and IFNλ levels in the supernatants of the infected cells. An interesting working model would be that, through its capacity to diffuse across membranes, DUOX2-derived H_2O_2 could modulate intracellular signals to regulate the production and/or secretion of IFNβ and IFNλ. A similar mechanism was previously implicated in the DUOX2-dependent regulation of NF-κB activity, and the thereof resulting IL-8 production and neutrophil recruitment [45]. The closely-related homolog of DUOX2, DUOX1 that is also expressed in AECs was previously shown to regulate EGFR-dependent signaling [46, 47]. Additionally, DUOX1-derived H_2O_2 was shown to regulate intracellular protein phosphatase activities [48, 49]. Although intracellular signaling modulation is a likely mechanism, regulation of IFN expression in our system is not due to altered transcriptional regulation, as IFNβ and IFNλ mRNA levels were not affected by the specific knockdown of DUOX2 using siRNA. Thus, it is unlikely that DUOX2-dependent production and/or secretion of IFNs involve the signaling cascades leading to NF-κB and ISGF3 TFs, which are key regulators of ISGs. It is noteworthy to mention that a recent publication has identified DUOX2 as a potential regulator of proinflammatory responses via shedding of the soluble TNFR in human AECs following TLR3 stimulation by poly (I:C) [50]. However, we did not observe an effect of DUOX2 knockdown on TNFR shedding during SeV infection (data not shown).

In conclusion, our study unveils a key function of DUOX2 in the establishment of a late antiviral state triggered by the synergistic autocrine/paracrine action of IFNβ and TNFα secreted during respiratory virus infection. Importantly, induction of the antiviral state by the combination of IFNβ and TNFα is specifically driven by a STAT2/IRF9-dependent, STAT1-independent non-canonical signaling pathway. Thus, our study reveals a novel antiviral signaling cascade that acts in a late fash-

ion compared with the classic ISGF3-dependent antiviral pathway.

Materials and Methods

Chemicals

The JAK inhibitor AG490 and the Tyk2-specific inhibitor Bayer-18 inhibitors were obtained from Enzo life Sciences and Symansis, respectively.

Cell culture

All media and supplements were purchased from Gibco, except for primary cell culture for which reagents were obtained from Clonetics. A549 cells (American Type Culture Collection, ATCC) were grown in F-12 nutrient mixture (Ham) medium supplemented with 10% heat-inactivated fetal bovine serum (HI-FBS) and 1% L-glutamine. Calu-3 cells (ATCC) were grown under submerged conditions in MEM medium supplemented with 10% HI-FBS, 1% L-glutamine, 1% sodium pyruvate and 1% non-essential amino acids. For Air-Liquid Culture (ALI), Calu-3 cells were plated at a density of 0.2×10^6 cells/cm^2 onto Greiner Transwell inserts coated with collagen VI (Sigma-Aldrich) for at least 16 h. Calu-3 cells were kept under submerged conditions for 48 h before medium in the apical compartment was removed. Cells were kept in ALI (ALI-Calu-3) culture for 10-14 days before conducting Transepithelial Electric Resistance (TEER) measurement with a Voltohmmeter (World Precision Instruments). Experiments were performed using ALI-Calu-3 having TEER measures equal to or higher than 800 Ω.cm^2. NHBE were obtained from Clonetics, cultured in BEGM medium (Clonetics) and used until maximum passage 3. Vero cells (ATCC) were cultured in DMEM medium supplemented with 10% HI-FBS and 1% L-glutamine.

Virus infections

SeV Cantell strain was obtained from Charles River Laboratories. The initial stock of RSV A2 strain was obtained from Advanced Biotechnologies, Inc. The initial stock of recombinant RSV encoding GFP (RecRSV-GFP) was a generous gift from Dr PL Collins (NIH, Bethesda). Amplification and purification of RSV and RecRSV-GFP was performed as previously described [51].

SeV infection was conducted at 40 hemagglutinin units (HAU) per 10^6 cells in serum free medium (SFM) for 2 h, after which the medium was supplemented with 10% HI-FBS. RSV or RecRSV-GFP infection was conducted at a MOI of 3 or 1, respectively, in medium containing 2% HI-FBS. Infection of ALI-Calu-3 was conducted the day after TEER measurement using viruses diluted in SFM (SeV) or 2% HI-FBS containing medium (RSV) and added apically onto Transwells. After 2 h, the apical medium was taken off and the infection was pursued in ALI condition. SeV infection of NHBE was conducted with 40 HAU/10^6 cells in BEGM.

Preparation of supernatant from infected cells

For generation of supernatant from SeV- or RSV-infected cells, A549 cells were infected as described above. At 2 hpi, the virus was taken off and the medium was replaced with Opti-MEM Reduced Serum media (Invitrogen). The infection was pursued for 22 h. Thereafter, the supernatant was harvested and cell debris eliminated by centrifugation. Where indicated, the supernatant was treated with UV for 20 min. To generate SN from A549 cells

treated with Z-VAD-FMK (Calbiochem), A549 cells were pretreated with 0.1 mM Z-VAD-FMK or DMSO (vehicle) for 1 h before infection. Z-VAD-FMK was present throughout the infection. For heat treatment, SN-SeV-UV was either left untreated or heated for 15 min at 80 °C.

Stimulation with recombinant cytokines

Recombinant IFNβ and TNFα (Feldan) were used at a final concentration of 1 000-5 000 IU/ml and 10-50 ng/ml, respectively, in F12 nutrient mixture (Ham), supplemented with 2% HI-FBS. Where indicated, cells were pretreated with AG490 (100 μM) or Bayer 18 (100 μM) or the corresponding vehicle DMSO for 1 h before cytokine stimulation.

Virus titration by plaque forming unit assay

The supernatant of A549 cells infected with RecRSV-GFP was harvested at 72 hpi. Serial dilutions of the supernatant were performed in DMEM (Gibco) containing 2% HI-FBS and used to infect confluent Vero cells for 2 h. Following this period, the medium was replaced with 1% methylcellulose in DMEM containing 2% HI-FBS. Infection was pursued for 7 days and fluorescent lysis plaques were visualized using a Typhoon apparatus (Molecular Dynamics) and counted using the ImageQuantTL colony counting analysis tool.

siRNA Transfection

RNAi oligonucleotides (see Supplementary information, Table S1 for sequences) were purchased from Dharmacon, except for siDUOX2(1), which was from Invitrogen. Transfection was performed as previously described [52] using Oligofectamine reagent (Invitrogen) and pursued for 48 h before viral infection or SN or cytokine stimulation.

Immunoblot analysis

Whole-cell extracts (WCE) were prepared on ice in Nonidet P-40 (Igepal; Sigma) lysis buffer [53], quantified by a Bradford protein assay (Bio-Rad), and resolved by SDS-PAGE, followed by immunoblot analysis. Proteins were immunodetected using anti-actin (Millipore), anti-ISG56 (IFIT1; Novus Biologicals), anti-IRF1 (Santa Cruz), anti-IRF9 (BD Transduction Laboratories), anti-parainfluenza (obtained from Dr J Hiscott, McGill University, Montreal, Canada), anti-PARP (Cell Signalling), anti-RSV (Chemicon International), anti-IκBα-P-Ser32, anti-IκBα anti-STAT1-P-Tyr701, anti-STAT2-P-Tyr690, anti-STAT1, anti-STAT2 (all from Cell Signaling), and anti-a-tubulin (Santa Cruz) antibodies diluted in phosphate-buffered saline (PBS) containing 0.5% Tween (Sigma Aldrich) and either 5% nonfat dry milk or 5% BSA (Sigma Aldrich). For DUOX2 and TNFRI immunodetection, WCE were prepared at room temperature in 125mM Tris/HCl (pH 6.8), 10% glycerol, 2% SDS and 0.1 M DTT followed by sonication (2 × 20 s) and heating to 70 °C for 10 min. WCE were quantified using a RC/DC protein assay (Bio-Rad). 150 μg WCE were resolved by SDS-PAGE. DUOX2 was immunodetected using the anti-DUOX1/2 specific antibodies previously described in [54]. TNFRI was immunodetected using the anti-TNFRI/TNFRSF1A antibodies (R&D Systems). The membranes were further incubated for 1 h with horseradish peroxidase (HRP)-conjugated secondary antibodies (Kirkegaard and Perry Laboratories or Jackson Immunoresearch Laboratories). Immunoreactive bands were visualized by enhanced chemiluminescence using the Western Lightning Chemiluminescence Reagent Plus (Perkin-Elmer Life Sciences) and detected using a LAS4000mini CCD camera apparatus (GE healthcare).

Quantitative RT-PCR (qRT-PCR) analyses

Total RNA was prepared using the RNAqueous-96 Isolation Kit (Ambion) following the manufacturer's instructions. Total RNA (1 μg) was subjected to reverse transcription using the QuantiTect Reverse Transcription Kit (Qiagen). PCR amplifications were performed with the Fast start SYBR Green Kit (Roche). Sequences of oligonucleotides (Invitrogen) are presented in Supplementary information, Table S2. Absence of genomic DNA contamination was analyzed using a reaction without reverse transcriptase. Detection was performed on a Rotor-Gene 3000 Real Time Thermal Cycler (Corbett Research). For *DUOX2*, *DUOXA2*, *IFNB, IL28, IL29, IFIT1*, *TNFα, β-actin* and *S9* genes qRT-PCR amplifications, standard curves of absolute quantification expressed as copy number and PCR efficiencies were obtained using serial dilutions of DUOX2-HA-pcDNA3.1 (a generous gift from Dr Grasberger, University of Michigan, Ann Harbor, MI, USA), DUOXA2-pCR4-TOPO, IL28-pCR4-TOPO, IL29-pCR4-TOPO, β-actin-pCR2.1-TOPO, ISG56-pCR2.1-TOPO, IFNβ-pCR2.1-TOPO, TNFα-pCR2.1-TOPO, and S9-pCR2.1-TOPO. Gene-specific absolute mRNA copy numbers were normalized to β-actin or S9 mRNA absolute copy numbers. For *IFNAR1* real-time amplification, serial dilutions of cDNA derived from IFNAR1 expressing A549 cells were used to determine primer efficiency and linearity of PCR reaction. IFNAR fold induction was calculated using the ΔΔ Cycle threshold (C_t) method [55].

Multiplex ELISA

SeV and RSV infections were conducted in Opti-MEM Reduced Serum media (Invitrogen). Where applicable, virus infection was performed 48 h post siRNA transfection. Fifty microlitres of SN were analyzed using the VeriPlex Human Interferon Multiplex ELISA (PBL Interferon) according to the manufacturer's instructions. The ELISA plate was imaged with the Q-View Imager and data analysis was performed using the Q-View Software (Quansys Biosciences).

H_2O_2 measurement

Extracellular H_2O_2 production was measured using homovanillic acid (HVA)-based fluorimetric assay as previously described [56]. Briefly, following stimulation, cells were incubated in Krebs-Ringer-Hepes solution containing 0.44 mM HVA and 0.1 mg/ml horseradish peroxidase for 2 h at 37 °C. Where indicated, catalase was added at 400 U/ml. At the end of the incubation period, fluorescence was quantified with an excitation wavelength of 315 nm and an emission wavelength of 425 nm on a HT Synergy (Biotek) plate reader. H_2O_2 concentration values were assigned using a H_2O_2 standard curve.

Statistical analyses

All quantification data are presented as the mean ± standard deviation (SD). Statistical significance for comparison was assessed using the Prism 5 software (GraphPad). Statistical significance was evaluated using the following P-values: $P < 0.05$ (*), $P < 0.01$ (**) or $P < 0.001$ (***).

Acknowledgments

References

1   Vareille M, Kieninger E, Edwards MR, Regamey N. The airway epithelium: soldier in the fight against respiratory viruses. *Clin Microbiol Rev* 2011; **24**:210-229.

2   Liu SY, Sanchez DJ, Cheng G. New developments in the induction and antiviral effectors of type I interferon. *Curr Opin Immunol* 2011; **23**:57-64.

3   Bae YS, Choi MK, Lee WJ. Dual oxidase in mucosal immunity and host-microbe homeostasis. *Trends Immunol* 2010; **31**:278-287.

4   Fischer H. Mechanisms and function of DUOX in epithelia of the lung. *Antioxid Redox Signal* 2009; **11**:2453-2465.

5   Harper RW, Xu C, Soucek K, Setiadi H, Eiserich JP. A reappraisal of the genomic organization of human Nox1 and its splice variants. *Arch Biochem Biophys* 2005; **435**:323-330.

6   Harper RW, Xu C, Eiserich JP, *et al*. Differential regulation of dual NADPH oxidases/peroxidases, Duox1 and Duox2, by Th1 and Th2 cytokines in respiratory tract epithelium. *FEBS Lett* 2005; **579**:4911-4917.

7   Fink K, Duval A, Martel A, Soucy-Faulkner A, Grandvaux N. Dual role of NOX2 in respiratory syncytial virus- and sendai virus-induced activation of NF-kappaB in airway epithelial cells. *J Immunol* 2008; **180**:6911-6922.

8   Luxen S, Belinsky SA, Knaus UG. Silencing of DUOX NADPH oxidases by promoter hypermethylation in lung cancer. *Cancer Res* 2008; **68**:1037-1045.

9   Grasberger H, Refetoff S. Identification of the maturation factor for dual oxidase. Evolution of an eukaryotic operon equivalent. *J Biol Chem* 2006; **281**:18269-18272.

10 Harcourt JL, Caidi H, Anderson LJ, Haynes LM. Evaluation of the Calu-3 cell line as a model of *in vitro* respiratory syncytial virus infection. *J Virol Methods* 2011; **174**:144-149.

11 Bartee E, Mohamed MR, Lopez MC, Baker HV, McFadden G. The addition of tumor necrosis factor plus beta interferon induces a novel synergistic antiviral state against poxviruses in primary human fibroblasts. *J Virol* 2009; **83**:498-511.

12 Yarilina A, Park-Min KH, Antoniv T, Hu X, Ivashkiv LB. TNF activates an IRF1-dependent autocrine loop leading to sustained expression of chemokines and STAT1-dependent type I interferon-response genes. *Nat Immunol* 2008; **9**:378-387.

13 Baetu TM, Kwon H, Sharma S, Grandvaux N, Hiscott J. Disruption of nf-kappab signaling reveals a novel role for nf-kappab in the regulation of tnf-related apoptosis-inducing ligand expression. *J Immunol* 2001; **167**:3164-3173.

14 Versteeg GA, Garcia-Sastre A. Viral tricks to grid-lock the type I interferon system. *Curr Opin Microbiol* 2010; **13**:508-516.

15 Mestan J, Brockhaus M, Kirchner H, Jacobsen H. Antiviral activity of tumour necrosis factor. Synergism with interferons and induction of oligo-2',5'-adenylate synthetase. *J Gen Virol* 1988; **69**:3113-3120.

16 Kimura A, Naka T, Nagata S, Kawase I, Kishimoto T. SOCS-1 suppresses TNF-alpha-induced apoptosis through the regulation of Jak activation. *Int Immunol* 2004; **16**:991-999.

17 Guo D, Dunbar JD, Yang CH, Pfeffer LM, Donner DB. Induction of Jak/STAT signaling by activation of the type 1 TNF receptor. *J Immunol* 1998; **160**:2742-2750.

18 Fujita T, Reis LFL, Watanabe N, Kimura Y, Taniguchi T, Vilcek J. Induction of the transcription factor IRF-1 and interferon-beta mRNAs by cytokines and activators of second-messenger pathways. *Proc Natl Acad Sci USA* 1989; **86**:9936-9940.

19 Tliba O, Tliba S, Da Huang C, *et al*. Tumor necrosis factor alpha modulates airway smooth muscle function via the autocrine action of interferon beta. *J Biol Chem* 2003; **278**:50615-50623.

20 Bluyssen HA, Levy DE. Stat2 is a transcriptional activator that requires sequence-specific contacts provided by stat1 and p48 for stable interaction with DNA. *J Biol Chem* 1997; **272**:4600-4605.

21 Kraus TA, Lau JF, Parisien JP, Horvath CM. A hybrid IRF9-STAT2 protein recapitulates interferon-stimulated gene expression and antiviral response. *J Biol Chem* 2003; **278**:13033-13038.

22 Hahm B, Trifilo MJ, Zuniga EI, Oldstone MB. Viruses evade the immune system through type I interferon-mediated STAT2-dependent, but STAT1-independent, signaling. *Immunity* 2005; **22**:247-257.

23 Sarkis PT, Ying S, Xu R, Yu XF. STAT1-independent cell type-specific regulation of antiviral APOBEC3G by IFN-alpha. *J Immunol* 2006; **177**:4530-4540.

24 Perry ST, Buck MD, Lada SM, Schindler C, Shresta S. STAT2 mediates innate immunity to Dengue virus in the absence of STAT1 via the type I interferon receptor. *PLoS Pathog* 2011; **7**:e1001297.

25 Lou YJ, Pan XR, Jia PM, *et al*. IRF-9/STAT2 (corrected) functional interaction drives retinoic acid-induced gene G expression independently of STAT1. *Cancer Res* 2009; **69**:3673-3680.

26 Linderholm AL, Onitsuka J, Xu C, Chiu M, Lee WM, Harper RW. All-trans retinoic acid mediates DUOX2 expression and function in respiratory tract epithelium. *Am J Physiol Lung Cell Mol Physiol* 2010; **299**:L215-L221.

27 Christophe-Hobertus C, Christophe D. Delimitation and functional characterization of the bidirectional THOX-DUOXA promoter regions in thyrocytes. *Mol Cell Endocrinol* 2010; **317**:161-167.

28 Ha EM, Lee KA, Seo YY, *et al*. Coordination of multiple dual oxidase-regulatory pathways in responses to commensal and

infectious microbes in drosophila gut. *Nat Immunol* 2009; **10**:949-957.

29 Hill T, 3rd, Xu C, Harper RW. IFNgamma mediates DUOX2 expression via a STAT-independent signaling pathway. *Biochem Biophys Res Commun* 2010; **395**:270-274.

30 Schneider D, Ganesan S, Comstock AT, *et al*. Increased cytokine response of rhinovirus-infected airway epithelial cells in chronic obstructive pulmonary disease. *Am J Respir Crit Care Med* 2010; **182**:332-340.

31 Chattoraj SS, Ganesan S, Faris A, Comstock A, Lee WM, Sajjan US. *Pseudomonas aeruginosa* suppresses interferon response to rhinovirus infection in cystic fibrosis but not in normal bronchial epithelial cells. *Infect Immun* 2011; **79**:4131-4145.

32 Comstock AT, Ganesan S, Chattoraj A, *et al*. Rhinovirus-induced barrier dysfunction in polarized airway epithelial cells is mediated by NADPH oxidase 1. *J Virol* 2011; **85**:6795-6808.

33 Swedan S, Musiyenko A, Barik S. Respiratory syncytial virus nonstructural proteins decrease levels of multiple members of the cellular interferon pathways. *J Virol* 2009; **83**:9682-9693.

34 Elliott J, Lynch OT, Suessmuth Y, *et al*. Respiratory syncytial virus NS1 protein degrades STAT2 by using the Elongin-Cullin E3 ligase. *J Virol* 2007; **81**:3428-3436.

35 Wright JM, Merlo CA, Reynolds JB, *et al*. Respiratory epithelial gene expression in patients with mild and severe cystic fibrosis lung disease. *Am J Respir Cell Mol Biol* 2006; **35**:327-336.

36 Wat D, Gelder C, Hibbitts S, *et al*. The role of respiratory viruses in cystic fibrosis. *J Cyst Fibros* 2008; **7**:320-328.

37 Ha EM, Oh CT, Bae YS, Lee WJ. A direct role for dual oxidase in Drosophila gut immunity. *Science* 2005; **310**:847-850.

38 Moskwa P, Lorentzen D, Excoffon KJ, *et al*. A novel host defense system of airways is defective in cystic fibrosis. *Am J Respir Crit Care Med* 2007; **175**:174-183.

39 Gattas MV, Forteza R, Fragoso MA, *et al*. Oxidative epithelial host defense is regulated by infectious and inflammatory stimuli. *Free Radic Biol Med* 2009; **47**:1450-1458.

40 Forteza R, Salathe M, Miot F, Forteza R, Conner GE. Regulated hydrogen peroxide production by Duox in human airway epithelial cells. *Am J Respir Cell Mol Biol* 2005; **32**:462-469.

41 Mikola H, Waris M, Tenovuo J. Inhibition of herpes simplex virus type 1, respiratory syncytial virus and echovirus type 11 by peroxidase-generated hypothiocyanite. *Antiviral Res* 1995; **26**:161-171.

42 Belding ME, Klebanoff SJ, Ray CG. Peroxidase-mediated virucidal systems. *Science* 1970; **167**:195-196.

43 Fischer AJ, Lennemann NJ, Krishnamurthy S, *et al*. Enhancement of respiratory mucosal antiviral defenses by the oxidation of iodide. *Am J Respir Cell Mol Biol* 2011; **45**:874-881.

44 Conner GE, Wijkstrom-Frei C, Randell SH, Fernandez VE, Salathe M. The lactoperoxidase system links anion transport to host defense in cystic fibrosis. *FEBS Lett* 2007; **581**:271-278.

45 Joo JH, Ryu JH, Kim CH, *et al*. Dual oxidase 2 is essential for the toll-like receptor 5-mediated inflammatory response in airway mucosa. *Antioxid Redox Signal* 2012; **16**:57-70.

46 Nakanaga T, Nadel JA, Ueki IF, Koff JL, Shao MX. Regulation of interleukin-8 via an airway epithelial signaling cascade. *Am J Physiol Lung Cell Mol Physiol* 2007; **292**:L1289-L1296.

47 Boots AW, Hristova M, Kasahara DI, Haenen GR, Bast A, van der Vliet A. ATP-mediated activation of the NADPH oxidase DUOX1 mediates airway epithelial responses to bacterial stimuli. *J Biol Chem* 2009; **284**:17858-17867.

48 Hirakawa S, Saito R, Ohara H, Okuyama R, Aiba S. Dual oxidase 1 induced by Th2 cytokines promotes STAT6 phosphorylation via oxidative inactivation of protein tyrosine phosphatase 1B in human epidermal keratinocytes. *J Immunol* 2011; **186**:4762-4770.

49 Kwon J, Shatynski KE, Chen H, *et al*. The nonphagocytic NADPH oxidase Duox1 mediates a positive feedback loop during T cell receptor signaling. *Sci Signal* 2010; **3**:ra59.

50 Yu M, Lam J, Rada B, Leto TL, Levine SJ. Double-stranded RNA induces shedding of the 34-kDa soluble TNFR1 from human airway epithelial cells via TLR3-TRIF-RIP1-dependent signaling: roles for dual oxidase 2- and caspase-dependent pathways. *J Immunol* 2011; **186**:1180-1188.

51 Yoboua F, Martel A, Duval A, Mukawera E, Grandvaux N. Respiratory syncytial virus-mediated NF-kappa B p65 phosphorylation at serine 536 is dependent on RIG-I, TRAF6, and IKK beta. *J Virol* 2010; **84**:7267-7277.

52 Sharma S, tenOever BR, Grandvaux N, Zhou GP, Lin R, Hiscott J. Triggering the interferon antiviral response through an IKK-related pathway. *Science* 2003; **300**:1148-1151.

53 Servant MJ, Grandvaux N, tenOever BR, Duguay D, Lin R, Hiscott J. Identification of the minimal phosphoacceptor site required for in vivo activation of interferon regulatory factor 3 in response to virus and double-stranded RNA. *J Biol Chem* 2003; **278**:9441-9447.

54 De Deken X, Wang D, Many MC, *et al*. Cloning of two human thyroid cDNAs encoding new members of the NADPH oxidase family. *J Biol Chem* 2000; **275**:23227-23233.

55 Dussault AA, Pouliot M. Rapid and simple comparison of messenger RNA levels using real-time PCR. *Biol Proced Online* 2006; **8**:1-10.

56 Rigutto S, Hoste C, Grasberger H, *et al*. Activation of dual oxidases Duox1 and Duox2: differential regulation mediated by camp-dependent protein kinase and protein kinase C-dependent phosphorylation. *J Biol Chem* 2009; **284**:6725-6734.

(**Supplementary information** is linked to the online version of the paper on the *Cell Research* website.)